

GROWING OF TUBES WITH A SMALL INNER DIAMETER FROM THE MELT BY THE STEPANOV METHOD

V. A. Borodin, A. V. Zhdanov, and
M. V. Yudin

UDC 536.421

A mathematical model is suggested for describing the growth of a crystal tube with a small inner diameter from the melt by the modified Stepanov method with the tube being affected by temperature pulses. The behavior of the inner and outer radii of the tube as a function of the amplitude and duration of temperature jumps is studied.

Introduction. Manufacture of tubes with a small inner diameter by the ordinary Stepanov method presents a number of difficulties caused by maintenance of a constant value of the thickness of the grown tube. Often the changes of the surrounding temperature are such that they lead to collapse of the internal cavity of the tube. Therefore, another type of shaper has been suggested; in this shaper, the inner diameter is created due to the presence of a thin cylindrical rod at the center with the upper end of the rod being located higher than the outer edge of the shaper.

This type of shaper requires studies associated with probabilistic power jumps of the generator which lead to changes in the surrounding temperature, which, in turn, causes such a behavior of the thickness of the grown tube where either capture of the shape-forming rod (freezing) by the crystal or break-off of the meniscus due to loss of its stability are possible. Based on the mathematical model suggested below, we studied the process of growth of a crystal under the action of a rectangular temperature pulse as a function of its amplitude and the duration of its effect.

Problem Formulation. First, we make some assumptions which allow us to considerably simplify the problem, viz., thermophysical parameters of the melt and the crystal are the same; heat liberated on the crystallization front slightly affects the total thermal field of the melt-crystal system; in temperature calculation, the change in the tube radii due to the effect of the temperature pulse can be neglected.

Under these assumption, the problem can be formulated as follows: during crystallization of a tube of length L with inner and outer radii R_1 and R_2 , respectively, at the speed of drawing V_0 the temperature field T^0 satisfies the heat-transfer equation

$$k_s \left(\frac{1}{r} \left(\frac{\partial}{\partial r} \left(r \frac{\partial T^0}{\partial r} \right) \right) + \frac{\partial^2 T^0}{\partial z^2} \right) - V_0 \rho_s c_s \frac{\partial T^0}{\partial z} = 0 \quad (1)$$

at the following boundary conditions: heat exchange with the surrounding medium, which has temperatures θ_1^0 and θ_2^0 , is specified on the inner and outer surfaces of the tube (Fig. 1):

$$-k_s \frac{\partial T^0}{\partial r} = h_s (T^0 - \theta_2^0) \Big|_{r=R_2}, \quad k_s \frac{\partial T^0}{\partial r} = h_s (T^0 - \theta_1^0) \Big|_{r=R_1}, \quad (2)$$

where

$$\theta_1^0 = T_1^0 + \frac{z}{L} (T_2^0 - T_1^0); \quad \theta_2^0 = T_3^0 + \frac{z}{L} (T_4^0 - T_3^0). \quad (3)$$

The temperatures

Institute of Solid Body Physics, Russian Academy of Sciences, Chernogolovka, Moscow Region, 142432, Russia; email: zhdan@issp.ac.ru. Translated from *Inzhenerno-Fizicheskii Zhurnal*, Vol. 77, No. 1, pp. 184–190, January–February, 2004. Original article submitted November 14, 2002; revision submitted July 7, 2003.

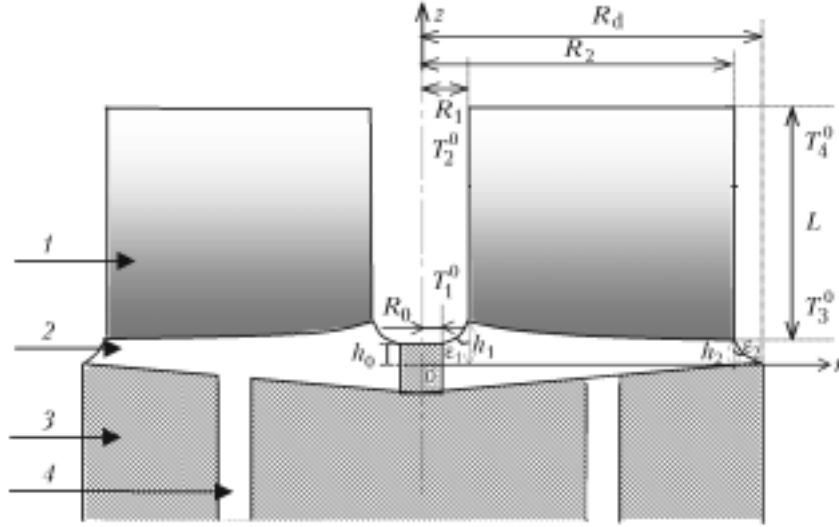


Fig. 1. Schematic of tube growth (system of the coordinates and the notations): 1) crystal; 2) melt; 3) shaper; 4) capillary channel.

$$T^0(r, 0) = T_0, \quad T^0(r, L) = T_c, \quad R_1 \leq r \leq R_2. \quad (4)$$

are specified at the lower and upper ends of the tube.

Under the effect of the temperature pulse, the temperature $T(r, z, \tau)$ in the crystal satisfies the following heat-conduction equation:

$$\frac{\partial T}{\partial \tau} = \frac{1}{r} \left(\frac{\partial}{\partial r} \left(r \frac{\partial T}{\partial r} \right) \right) + \frac{\partial^2 T}{\partial z^2}, \quad \tau = at, \quad a = \frac{k_s}{c_s \rho_s}, \quad (5)$$

with the boundary conditions

$$\begin{aligned} -k_s \frac{\partial T}{\partial r} &= h_s (T - \theta_2) \Big|_{r=R_2}, \quad k_s \frac{\partial T}{\partial r} = h_s (T - \theta_1) \Big|_{r=R_1}, \\ T(r, 0, \tau) &= T_0, \quad T(r, L, \tau) = T_c, \quad R_1 \leq r \leq R_2, \end{aligned} \quad (6)$$

and the initial condition

$$T(r, z, 0) = T^0(r, z). \quad (7)$$

The temperatures θ_1 and θ_2 are assumed to change with time according to the laws

$$\begin{aligned} \theta_1 &= T_1^0 + \frac{z}{L} (T_2^0 - T_1^0) + A [\eta (t - \tau_1) - \eta (t - \tau_2)], \\ \theta_2 &= T_3^0 + \frac{z}{L} (T_4^0 - T_3^0) + B [\eta (t - \tau_1) - \eta (t - \tau_2)]. \end{aligned} \quad (8)$$

The behavior of the inner $r_1(z)$ and outer $r_2(z)$ radii is found from the differential equations

$$\dot{r}_1 = -(V_0 - \dot{h}_1) \tan(\varepsilon_1 - \varepsilon_0), \quad r_1(0) = R_1; \quad \dot{r}_2 = (V_0 - \dot{h}_2) \tan(\varepsilon_2 - \varepsilon_0), \quad r_2(0) = R_2. \quad (9)$$

Moreover, $r_1(z)$ and $r_2(z)$ satisfy the capillary Laplace equations which can be obtained by minimization of the functional $J(r_1, r_2)$, which, to an accuracy of a constant, is the potential energy of the melt meniscus

$$J(r_1, r_2) = 2\pi\sigma \int_{h_0}^{h_1} r_1 \sqrt{1+r_1'^2} dz + 2\pi\sigma \int_0^{h_2} r_2 \sqrt{1+r_2'^2} dz + \pi\rho_m g \int_0^{h_2} (z+H) r_2^2 dz - \pi\rho_m g \int_{h_0}^{h_1} (z+H) r_1^2 dz. \quad (10)$$

Then, the equations and boundary conditions, which describe the profile curves of the menisci r_1 and r_2 , take on the following form:

$$\begin{aligned} \sigma \left(\frac{r_2''}{(1+r_2'^2)^{3/2}} - \frac{1}{r_2 \sqrt{1+r_2'^2}} \right) - \rho_m g (z+H) = 0, \quad r_2(0) = R_d, \quad r_2(h_2) = R_2; \\ \sigma \left(\frac{r_1''}{(1+r_1'^2)^{3/2}} - \frac{1}{r_1 \sqrt{1+r_1'^2}} \right) + \rho_m g (z+H) = 0, \quad r_1(h_0) = R_0, \quad r_1(h_1) = R_1, \end{aligned} \quad (11)$$

where the prime indicates the derivative with respect to z .

With the temperature field $T(r, z, t)$ being known, we can determine the position of the crystallization front $z = f(r, t)$ by drawing the isotherm of the melting temperature

$$T(r, z, t) = T_m. \quad (12)$$

Consequently, the heights of the menisci h_1 and h_2 are just their values at $r = R_1$ and $r = R_2$:

$$h_1 = f(R_1), \quad h_2 = f(R_2). \quad (13)$$

Determining the radii $r_1(z)$ and $r_2(z)$ from Eqs. (11), we thus can find the angles ε_1 and ε_2 .

Solution of the Problem Posed and Discussion of the Results. The solution of problem (1)–(4) for determination of the initial temperature field $T^0(r, z)$ can be found in [1, 2]. We present solution (5)–(7) in the form of the sum

$$T = T_1 + T^*, \quad (14)$$

where

$$\begin{aligned} T^* = \lambda \frac{\theta_1^0 - \theta_2^0}{\omega_1 + \omega_2} \ln r \frac{\theta_1^0 \omega_2 - \theta_2^0 \omega_1}{\omega_1 + \omega_2} + \left[\lambda \frac{A - B}{\omega_1 + \omega_2} \ln r + \frac{A\omega_2 + B\omega_1}{\omega_1 + \omega_2} \right] [\eta(t - \tau_1) - \eta(t - \tau_2)]; \\ \omega_1 = \frac{1}{R_1} - \lambda \ln R_1; \quad \omega_2 = \frac{1}{R_2} - \lambda \ln R_2; \quad \lambda = h_s/k_s. \end{aligned} \quad (15)$$

We substitute (14) into Eqs. (5)–(7) and apply the Laplace transform to T_1 . Then for \tilde{T}_1 , which is the Laplace transformation of the function T_1 , we have

$$\begin{aligned} \frac{1}{r} \left(\frac{\partial}{\partial r} \left(r \frac{\partial \tilde{T}_1}{\partial r} \right) \right) + \frac{\partial^2 \tilde{T}_1}{\partial z^2} - p \tilde{T}_1 = F(r, z, p), \quad F(r, z, p) = p \tilde{T}^* - T^0, \\ -k_s \frac{\partial \tilde{T}_1}{\partial r} = h_s \tilde{T}_1 \Big|_{r=R_2}, \quad k_s \frac{\partial \tilde{T}_1}{\partial r} = h_s \tilde{T}_1 \Big|_{r=R_1}, \end{aligned} \quad (16)$$

$$\tilde{T}_1(r, 0, p) = \tilde{T}_0 - \tilde{T}^*(r, 0), \quad \tilde{T}_1(r, L, p) = \tilde{T}_c - \tilde{T}^*(r, L).$$

The obtained problem (16) admits separation of variables and its solution can be presented in the form

$$\tilde{T}_1(r, z, p) = \sum_{k=1}^{\infty} \tilde{Z}_k(z, p) X_k(r). \quad (17)$$

Here the functions $X_k(t)$ are determined by the equalities

$$X_k = \frac{D_k(r)}{\|D_k\|}, \quad D_k = D \left(\frac{\mu_k}{R_2} r \right) = J_0 \left(\frac{\mu_k}{R_2} r \right) + \gamma(\mu_k) N_0 \left(\frac{\mu_k}{R_2} r \right), \quad (18)$$

$$D = J_0(r) + \gamma(\mu) N_0(r).$$

Eigenvalues of μ_k are the solutions of the algebraic equation

$$\begin{vmatrix} \mu J_1(\mu) - k J_0(\mu) & \mu N_1(\mu) - k N_0(\mu) \\ \mu J_1 \left(\mu \frac{R_1}{R_2} \right) + k J_0 \left(\mu \frac{R_1}{R_2} \right) & \mu N_1 \left(\mu \frac{R_1}{R_2} \right) + k N_0 \left(\mu \frac{R_1}{R_2} \right) \end{vmatrix} = 0, \quad (19)$$

where

$$k = \frac{h_s R_2}{k_s}; \quad \gamma(\mu_k) = - \frac{\mu_k J_1(\mu_k) - k J_0(\mu_k)}{\mu_k N_1(\mu_k) - k N_0(\mu_k)}. \quad (20)$$

The square of the norm of the function D_k is found as

$$\|D_k\|^2 = \frac{(k^2 + \mu_k^2)}{2\lambda_k} \left[D^2(\mu_k) - \left(\frac{R_1}{R_2} \right)^2 D^2 \left(\mu_k \frac{R_1}{R_2} \right) \right], \quad \lambda_k = (\mu_k / R_2)^2. \quad (21)$$

We introduce the following notation

$$M_k^{(1)} = T_m m_k - \lambda \frac{T_1^0 - T_3^0}{\omega_1 + \omega_2} l_k - \frac{T_1^0 \omega_2 + T_3^0 \omega_1}{\omega_1 + \omega_2} m_k, \quad (22)$$

$$M_k^{(2)} = T_c m_k - \lambda \frac{T_2^0 - T_4^0}{\omega_1 + \omega_2} l_k - \frac{T_2^0 \omega_2 + T_4^0 \omega_1}{\omega_1 + \omega_2} m_k, \quad (23)$$

$$L_k = \left[\lambda \frac{A - B}{\omega_1 + \omega_2} l_k + \frac{A \omega_2 + B \omega_1}{\omega_1 + \omega_2} m_k \right], \quad (24)$$

$$m_k = \frac{k}{\lambda_k \|D_k\|} = \left[D(\mu_k) + \frac{R_1}{R_2} D \left(\mu_k \frac{R_1}{R_2} \right) \right], \quad (25)$$

$$l_k = \frac{1}{\lambda_k \|D_k\|} \left[k D(\mu_k) \ln R_2 + k \frac{R_1}{R_2} D \left(\mu_k \frac{R_1}{R_2} \right) \ln R_1 + D(\mu_k) - D \left(\mu_k \frac{R_1}{R_2} \right) \right], \quad (26)$$

$$G_k^{(1)} = \frac{\left(b_k^0 + \frac{c_k^0}{\lambda_k} \right) \exp\left(-\frac{L(\eta_k + \chi)}{2} \right) - \left(a_k^0 + \frac{c_k^0}{\lambda_k} \right)}{\exp(-\eta_k L) - 1}, \quad (27)$$

$$G_k^{(2)} = \frac{\left(b_k^0 + \frac{c_k^0}{\lambda_k} \right) \exp\left(\frac{L(\eta_k - \chi)}{2} \right) - \left(a_k^0 + \frac{c_k^0}{\lambda_k} \right)}{\exp(-\eta_k L) - 1}, \quad (28)$$

$$\chi = \frac{V_0 \rho_s c_s}{k_s}; \quad \eta_k = \sqrt{\chi^2 + 4\lambda_k}; \quad a_k^0 = \delta_1 m_k + \gamma_1 l_k. \quad (29)$$

The coefficients b_k^0 are calculated by the same formulas as a_k^0 with the exception that δ_2 and γ_2 must be taken instead of δ_1 and γ_1 . The coefficients δ_i and γ_i ($i = 1, 2$) are determined by the following expressions:

$$\delta_1 = T_0 - \frac{T_1^0 \omega_2 + T_3^0 \omega_1}{\omega_1 + \omega_2}, \quad \gamma_1 = -\lambda \frac{T_3^0 - T_1^0}{\omega_1 + \omega_2}, \quad \delta_2 = T_c - \frac{T_2^0 \omega_2 + T_4^0 \omega_1}{\omega_1 + \omega_2}, \quad \gamma_2 = -\lambda \frac{T_4^0 - T_2^0}{\omega_1 + \omega_2}. \quad (30)$$

The coefficients c_k^0 are found from the formulas

$$c_k^0 = \frac{\chi}{\lambda_k \|D_k\|} = \left\{ [\alpha (k \ln R_2 + 1) + \beta k] D(\mu_k) + \left[\alpha \left(k \frac{R_1}{R_2} \ln R_1 - 1 \right) + \beta \frac{R_1}{R_2} k \right] D\left(\mu_k \frac{R_1}{R_2} \right) \right\}, \quad (31)$$

where

$$\alpha = \lambda \frac{T_1^0 - T_2^0 - T_3^0 + T_4^0}{L(\omega_1 + \omega_2)}; \quad \beta = \frac{(T_2^0 - T_1^0)\omega_2 + (T_4^0 - T_3^0)\omega_1}{L(\omega_1 + \omega_2)}. \quad (32)$$

Using the known theorems of inversion of the Laplace transform which are applied to the functions $\tilde{Z}_k(z, p)$, we find their originals $Z_k(z, t)$:

$$\begin{aligned} Z_k = & 2\pi G_k^{(1)} \sum_{j=1}^{\infty} (-1)^{j+1} j \frac{\exp\left(\frac{\chi - \eta_k}{2} L \right) \sin \frac{j\pi z}{L} + \sin \frac{j\pi(L-z)}{L}}{L^2 \left(\frac{j^2 \pi^2}{L^2} + \left(\frac{\chi - \eta_k}{2} \right)^2 \right)} \exp \left[- \left(\frac{j^2 \pi^2}{L^2} + \lambda_k \right) at \right] + \\ & + 2\pi G_k^{(2)} \sum_{j=1}^{\infty} (-1)^{j+1} j \frac{\exp\left(\frac{\chi - \eta_k}{2} L \right) \sin \frac{j\pi z}{L} + \sin \frac{j\pi(L-z)}{L}}{L^2 \left(\frac{j^2 \pi^2}{L^2} + \left(\frac{\chi - \eta_k}{2} \right)^2 \right)} \exp \left[- \left(\frac{j^2 \pi^2}{L^2} + \lambda_k \right) at \right] + \\ & + 2 \frac{c_k^{(0)}}{\lambda_k} \sum_{j=1}^{\infty} (-1)^j \frac{\sin \frac{j\pi z}{L} + \sin \frac{j\pi(L-z)}{L}}{j\pi} \exp \left[- \left(\frac{j^2 \pi^2}{L^2} + \lambda_k \right) at \right] + \end{aligned}$$

$$\begin{aligned}
& + \frac{2}{\pi} L_k \left\{ \sum_{j=1}^{\infty} (-1)^j \frac{\sin \frac{j\pi}{L} z + \sin \frac{j\pi}{L} (L-z)}{j} \left(\exp \left[- \left(\left(\frac{j\pi}{L} \right)^2 + \lambda_k \right) (t - \tau_1) a \right] \eta (t - \tau_1) - \right. \right. \\
& \quad \left. \left. - \exp \left[- \left(\left(\frac{j\pi}{L} \right)^2 + \lambda_k \right) (t - \tau_2) a \right] \eta (t - \tau_2) \right) \right\} + \\
& + M_k^{(1)} \left\{ \frac{\sinh \sqrt{\lambda_k} (L-z)}{\sinh \sqrt{\lambda_k} L} + \frac{2\pi}{L^2} \sum_{j=1}^{\infty} (-1)^j \frac{j \sin \frac{j\pi}{L} (L-z)}{\lambda_k + \left(\frac{j\pi}{L} \right)^2} \exp \left(- \left(\left(\frac{j\pi}{L} \right)^2 + \lambda_k \right) at \right) \right\} + \\
& + M_k^{(2)} \left\{ \frac{\sinh \sqrt{\lambda_k} z}{\sinh \sqrt{\lambda_k} L} + \frac{2\pi}{L^2} \sum_{j=1}^{\infty} (-1)^j \frac{j \sin \frac{j\pi}{L} z}{\lambda_k + \left(\frac{j\pi}{L} \right)^2} \exp \left(- \left(\left(\frac{j\pi}{L} \right)^2 + \lambda_k \right) at \right) \right\} - \\
& - L_k \left\{ \frac{\sinh \sqrt{\lambda_k} (L-z) + \sinh \sqrt{\lambda_k} z}{\sinh \sqrt{\lambda_k} L} \eta (t - \tau_1) + \frac{2\pi}{L^2} \sum_{j=1}^{\infty} (-1)^j j \frac{j \left(\sin \frac{j\pi}{L} (L-z) + \sin \frac{j\pi}{L} z \right)}{\lambda_k + \left(\frac{j\pi}{L} \right)^2} \times \right. \\
& \quad \left. \times \exp \left(- \left(\left(\frac{j\pi}{L} \right)^2 + \lambda_k \right) a (t - \tau_1) \right) \eta (t - \tau_1) \right\} + \\
& + L_k \left\{ \frac{\sinh \sqrt{\lambda_k} (L-z) + \sinh \sqrt{\lambda_k} z}{\sinh \sqrt{\lambda_k} L} \eta (t - \tau_2) + \frac{2\pi}{L^2} \sum_{j=1}^{\infty} (-1)^j j \frac{j \left(\sin \frac{j\pi}{L} (L-z) + \sin \frac{j\pi}{L} z \right)}{\lambda_k + \left(\frac{j\pi}{L} \right)^2} \times \right. \\
& \quad \left. \times \exp \left(- \left(\left(\frac{j\pi}{L} \right)^2 + \lambda_k \right) a (t - \tau_2) \right) \eta (t - \tau_2) \right\}. \tag{33}
\end{aligned}$$

Then we can find the temperature $T_1(r, z, t)$:

$$T_1(r, z, t) = \sum_{k=1}^{\infty} Z_k(z, t) X_k(r), \tag{34}$$

and, consequently, according to (14), the temperature distribution in the crystal $T(r, z, t)$.

The inner and outer radii of the tube, which vary under the effect of the temperature jump, can be found by Eqs. (9):

$$r_1(t) = R_1 - \int_{\tau_1}^t (V_0 - \dot{h}_1) \tan(\varepsilon_1 - \varepsilon_0) dt, \quad r_2(t) = R_2 + \int_{\tau_1}^t (V_0 - \dot{h}_2) \tan(\varepsilon_2 - \varepsilon_0) dt. \tag{35}$$

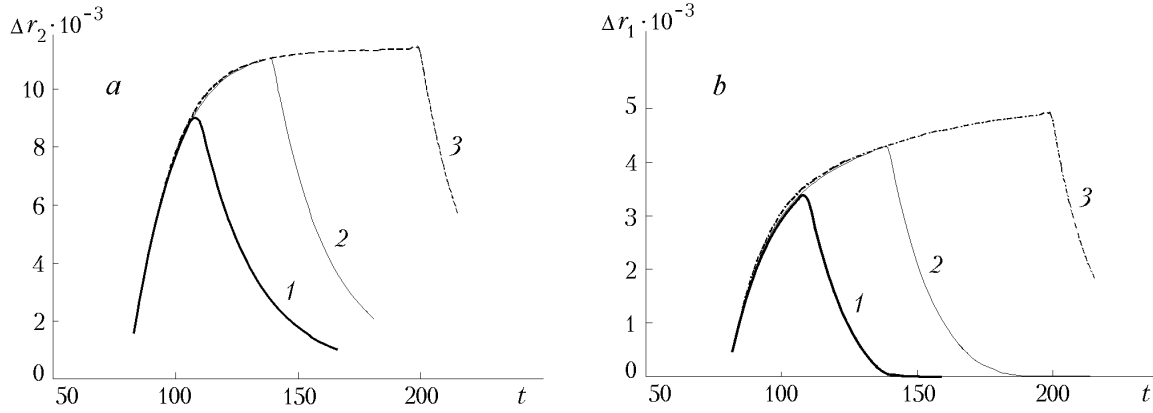


Fig. 2. The outer Δr_2 (a) and inner Δr_1 (b) radii as a function of time of the temperature pulse: 1) $\Delta\tau = 30$ sec; 2) 60; 3) 120. $\Delta r_1, \Delta r_2$, cm; t , sec.

If the coordinates of the catching points of the meniscus with the inner and outer radii $r_1(z)$ and $r_2(z)$ are specified, the boundary-value problems (11) allow one to completely determine $r_1(z)$ and $r_2(z)$ and, thus, values of the angles ε_1 and ε_2 . These problems were solved by the Runge–Kutta method by "shooting" from the points (R_1, h_1) and (R_2, h_2) to the edges of the rod and the shaper, respectively.

We denote changes of the inner and outer radii of the tube relative to their initial values R_1 and R_2 in terms of $\Delta r_1(t)$ and $\Delta r_2(t)$:

$$\Delta r_1(t) = \int_{\tau_1}^t (V_0 - \dot{h}_1) \tan(\varepsilon_1 - \varepsilon_0) dt, \quad \Delta r_2(t) = \int_{\tau_1}^t (V_0 - \dot{h}_2) \tan(\varepsilon_2 - \varepsilon_0) dt. \quad (36)$$

The results of the calculations are given in Fig. 2 at the following parameters of growth: rate of drawing $V_0 = 3.3 \cdot 10^{-3}$ cm/sec; amplitudes of the temperature jump $A = \pm 5^\circ\text{C}$, $B = \pm 8^\circ\text{C}$; $R_1 = 0.08$ cm; $R_2 = 2$ cm; $R_0 = 0.065$ cm; $h_0 = 0.05$ cm; $L = 5.0$ cm; $T_1^0 = 2000^\circ\text{C}$; $T_2^0 = 1540^\circ\text{C}$; $T_3^0 = 1950^\circ\text{C}$; $T_4^0 = 1500^\circ\text{C}$; $T_c = 1550^\circ\text{C}$; $T_0 = 2100^\circ\text{C}$. The temperature conditions and the geometric parameters of the shaper are selected such that at the initial instant of time the angles ε_1 and ε_2 are equal to the angle of growth $\varepsilon_0 = 11^\circ$. It is seen from the figure that the behaviors of the inner and outer radii are similar in shape, although the maximum value of Δr_2 exceeds the largest value of Δr_1 1.5–2.5 times. Thus, if the maximum change in Δr_1 is 0.005 cm, then the highest change in Δr_2 is equal to 0.0117 cm. Moreover, if the time of pulse effect is rather large (more than 1 min), then, beginning with certain times, Δr_1 and Δr_2 virtually do not change. A similar picture is observed with a positive temperature pulse with the only difference being that Δr_1 and Δr_2 are negative, i.e., the tube thickness will decrease.

We revealed two main types of behavior of Δr_1 and Δr_2 : (1) $\Delta r_1 = R_1 - R_0$ at a certain value of time t — the crystal is frozen to the rod; (2) always $\Delta r_1 < R_1 - R_0$ (at any value of $\Delta\tau$), and then the process crystallization changes over to a new stationary regime of growth with different values of the inner and outer radii R_1 and R_2 .

Of course, realization of one way or another of development of the process depends on the amplitudes of the temperature effect A and B and each specific case needs its own calculations. For example, for the case given in Fig. 2 ($A = -5^\circ\text{C}$, $B = -8^\circ\text{C}$), there is no freezing of the crystal to the rod during any period of action of the temperature pulse. If the temperature changes are $A < -10^\circ\text{C}$ and $B < -15^\circ\text{C}$, the crystal freezes to the rod in less than 30 sec.

We now refer to the case where the pulse is positive ($A > 0$, $B > 0$). In this case, both the change of the process over a new stationary regime of growth (with a large duration of the pulse effect $\Delta\tau$ and at rather small A and B) (a) and (b) break-off of the meniscus due to loss of its stability are possible. The latter is reduced to the investigation of the second variation $\delta^2 J$ of the functional $J(r_1, r_2)$: if $\delta^2 J > 0$, the meniscus is stable and it is unstable when $\delta^2 J < 0$.

According to formula (10), we write $\delta^2 J$ in the form

$$\delta^2 J = (L_1 y_1, y_1) \xi^2 + (L_2 y_2, y_2) \eta^2, \quad (37)$$

where

$$L_q(y) = -\frac{d}{dz}(R_q y') + P_q y; \quad (38)$$

$$R_q = \frac{1}{2} \frac{r_q}{(1+r_q^2)^{3/2}}; \quad P_q = \frac{1}{2} \left((-1)^{q+1} \frac{\rho_m g}{\sigma} (z+H) - \frac{r_q''}{(1+r_q^2)^{3/2}} \right); \quad q = 1, 2, \quad (39)$$

and ξ and η are arbitrary, rather small, quantities.

Since $R_q > 0$, finally the problem is reduced to revealing whether the operators L_1 and L_2 are positive determined. The answer to this question can be given by calculation of the eigenvalues of these operators: if any of them is not positive, the meniscus is unstable. For determination we use the Ritz method [3]. We represent approximations of the n th order $\phi_n^{(q)}$ to the eigenvectors $\phi_n^{(q)}$ of the operators L_1 and L_2 as

$$\phi_n^{(q)} = \sum_{k=1}^n b_k^{(q)} e_k^{(q)}, \quad (40)$$

where

$$e_k^{(1)} = \sqrt{\frac{2}{h_1 - h_0}} \sin \frac{k\pi}{h_1 - h_0} (z - h_0); \quad e_k^{(2)} = \sqrt{\frac{2}{h_2}} \sin \frac{k\pi}{h_2} z. \quad (41)$$

Then approximations of the n th order $\bar{\lambda}_q$ to the eigenvalues λ_q are found from the algebraic equation

$$|\Lambda_q - \bar{\lambda}_q I| = 0, \quad (42)$$

where Λ_q is the matrix

$$\Lambda_q = \begin{bmatrix} e_i^{(q)}, e_j^{(q)} \end{bmatrix}, \quad i, j = 1, \dots, n;$$

$$\begin{bmatrix} e_k^{(1)}, e_j^{(1)} \end{bmatrix} = \int_0^{h_2} \left(R_1 e_k'^{(1)} e_j'^{(1)} + P_1 e_k^{(1)} e_j^{(1)} \right) dz; \quad \begin{bmatrix} e_k^{(2)}, e_j^{(2)} \end{bmatrix} = \int_{h_0}^{h_1} \left(R_2 e_k'^{(2)} e_j'^{(2)} + P_2 e_k^{(2)} e_j^{(2)} \right) dz.$$

The calculations showed that even at rather large amplitudes A and B the eigenvalues λ_q are positive, with the first eigenvalue of the operator L_2 being much smaller than that of the operator L_1 . This indicates that under the effect of temperature pulses within a wide range of their variation the melt meniscus is stable and, moreover, the outer surface of the melt meniscus is less stable than the inner surface.

Conclusions. Based on the suggested mathematical model of growth of crystal tubes with a small inner diameter by the modified Stepanov method and the calculations according to it we showed the existence of critical values of the negative amplitudes of temperature pulses at which the crystal is frozen to the rod. In the case of the positive amplitudes within a wide range of their variation, the meniscus does not break off. Consequently, a decrease in the power of the generator is the most negative factor, which is the first to be reckoned with.

NOTATION

A and B , values of the temperature jumps of the surrounding media inside and outside the growing tube; c_s , specific heat capacity; g , free-fall acceleration; h_0 , rod height; h_1 and h_2 , heights of the melt meniscus from the inner

and outer sides of the tube; h_s , heat-transfer coefficient; H , distance from the level of the melt in the crucible to the edge of the shaper; J_0 and N_0 , Bessel functions of first and second kind; k_s , thermal conductivity; L , tube length; p , parameter of the Laplace transform; r , z , cylindrical coordinates; r_1 and r_2 , current values of the inner and outer radii of the tube; R_0 , radius of the rod; R_1 and R_2 , inner and outer radii of the tube; R_d , radius of the shaper; t , time; T_1 , T^* , parts of temperature T ; T_0 and T_c , temperature on the lower and upper ends of the crystal; T_m , temperature of crystal melting; T^0 , initial temperature of the tube; T_1^0 , T_2^0 , and T_3^0 , T_4^0 , temperatures which determine the state of the surrounding medium inside and outside the tube; \tilde{T} , Laplace transform of T ; V_0 , speed of drawing; ε_0 , angle of growth; ε_1 and ε_2 , angles between the profile curves of the menisci r_1 and r_2 and the axis z ; $\eta(t)$, Heaviside function; θ_1 , θ_2 and θ_1^0 , θ_2^0 , temperatures of the surrounding medium inside and outside the growing tube in nonstationary and stationary growth; ρ_m , density of the melt; ρ_c , crystal density; σ , coefficient of surface tension of the melt; τ , quantity related to time t ; τ_1 and τ_2 , final and initial instants of time of temperature jump action. Subscripts: s, solid; d, shaper; m, melt; c, crystal.

REFERENCES

1. A. V. Zhdanov and L. P. Nikolaeva, Thermal Stresses in Tubes, Produced from a Melt by the Stepanov Method, During Their Cooling, *Inzh.-Fiz. Zh.*, **68**, No. 1, 86–95 (1995).
2. A. V. Zhdanov, V. A. Borodin, and L. P. Nikolaeva, Thermoelastic Stresses in Tubes Produced from a Melt by Stepanov's Method, *Inzh.-Fiz. Zh.*, **64**, No. 3, 469–475 (1993).
3. S. G. Mikhlin, *Variational Methods in Mathematical Physics* [in Russian], Mir, Moscow (1970).